



# Solidification phenomena in creep resistant 9Cr weld metals and their implications on mechanical properties

A. Nitsche<sup>1</sup>

Received: 23 August 2019 / Accepted: 7 February 2020 / Published online: 14 February 2020  
© The Author(s) 2020

## Abstract

Martensitic 9% Cr steels play an important role in the implementation of modern and efficiency-enhanced power generation technologies. In the presented study, metallurgical solidification phenomena in heat-resistant 9% Cr filler metals and their effects on the mechanical properties of the weld metal were analysed. The focus was on welded joints of steel grades P91 and CB2, which were welded with flux-cored wires. The investigation of welded joints and weld metals in the creep-damaged and unloaded condition provided detailed insights into the formation and development of inhomogeneous areas. The microstructure of the individual weld metals was characterized in detail in the as-welded and in the heat-treated condition. It became apparent that inhomogeneities were formed in large areas of the weld metal. In particular, EDX measurements made it possible to explain these solidification phenomena and trace their development within the manufacturing process of the welded joints. It was found that even a slight uneven distribution of chromium and a diffusion of carbon caused extensive negative effects on the development of weld metal microstructures. In addition, the influence of these microstructural inhomogeneities on both the mechanical weld metal properties and the creep rupture strength is discussed. Finally, test welds were performed to optimize the microstructure of the flux-cored wire weld metal and possibilities to avoid microstructural inhomogeneities were derived. The results show that the short-term and long-term properties of the weld metal are affected by the inhomogeneous areas within the weld metal. In summary, it can be assumed that for steel grades P91 and CB2 the safety of plants in high-temperature operation is not endangered.

**Keywords** 9Cr weld metal · Flux-cored wire · White bands · Inhomogeneities · Creep resistant steel · Grade 91 · CB2

## 1 Introduction

It is generally accepted that Type IV cracking for subcritical heat-treated welds of 9% Cr steels (below phase transition temperature  $A_{c1}$ ) is the primary limiting factor for the long-term service life under creep loading [1]. Under the same load conditions, the creep strength of welded joints decreases significantly compared to the base metal due to the onset of Type IV damage [2]. However, crack formation in welded joints of 9% Cr steels depends on the test and operating conditions. For welded joints of the steels P91 [3] and P92 [4], creep tests

have shown that the fracture of the specimens under high load occurs in the weld metal (Type I) and is shifted into the heat affected zone (HAZ) at lower load and longer test duration (Type IV). Falat et al. [5] describe a similar result for TIG welds in CB2 heat-resistant steel. However, such a shift of the fracture location from the weld metal into the HAZ does not always occur. A displacement of the fracture from the base metal into the HAZ is also possible as creep tests on P92 [6] and CB2 [7] welded joints show.

Zhang [8], Zhang et al. [9] and Allen et al. [10] reported creep damage occurring within P91 and P92 weld metals. Among other things, so-called white bands, which were formed between the individual welding layers, have been identified as the cause of damage. In [10], a welded joint of the martensitic cast material HCM12A (T/P122: 12Cr-2 W-0,4Mo-1Cu-VNb) was investigated, which was produced with a P92 filler metal. The creep failure of the P92 weld metal was attributed to two causes. On the one hand, cracks that moved along columnar grain boundaries occurred within the weld

---

Recommended for publication by Commission IX - Behaviour of Metals Subjected to Welding

---

✉ A. Nitsche  
alexander.nitsche@mb.tu-chemnitz.de

<sup>1</sup> Institute of Joining and Assembly, Technische Universität Chemnitz, Reichenhainer Straße 70, 09126 Chemnitz, Germany

beads (interdendritic). On the other hand, damage was found in the area of the “white bands” (between the weld layers). The total damage was caused by the combination of the individual crack phenomena. Zhang et al. [9] also described the “white bands” with regard to creep strength as a detrimental factor, since they cause Type I cracks in the columnar weld metal areas to grow together and accelerate the damage, in particular under a load transverse to the weld seam.

According to [8, 9], the “white bands” can be described as follows. Within these zones – typically 100 to 200- $\mu\text{m}$  wide – a reduced number of stabilizing precipitates is found. Furthermore, the microstructure is completely recrystallized. The microhardness within the “white bands” is significantly reduced compared to the surrounding martensitic area. Within the “white bands”, there is a reduced Cr, C, Mn and Mo content. The clearer (brighter) the appearance of these zones, which are depleted of precipitates, the lower is their C and Cr content. The lack of stabilizing effect of precipitates in conjunction with the absence of martensite lath structure and the formation of large, soft ferrite grains results in a significant reduction in the creep strength of the inhomogeneous areas [9].

After welding as well as in the heat-treated condition, no “white bands” were present within the P91 manual metal arc (MMA) weld metal [9]. However, it was determined that after welding thin, elongated areas with a reduced Cr content had been formed in the area of fusion lines. At the same time, the carbon had a homogeneous distribution [8]. Zhang refers in his explanation of the “white band” formation to investigations by Savage et al. [11]. Savage et al. [11] described the formation of an unmixed zone at the fusion line of two weld layers. Due to the laminar flow in the area of the fusion line of the molten pool, the molten core rod and the molten powder components of the stick electrode coating are insufficiently mixed. This leads to the conclusion that the measured gradients of the Cr content result from the insufficient flow and mixing conditions. Under creep loading, the locally reduced Cr content enables the carbides to dissolve in these areas, and the carbon diffuses outwards into areas with a higher Cr content. Carbide dissolution also promotes recrystallization. Due to the comparatively narrow low-Cr zones (approx. 100–200  $\mu\text{m}$ ), only short diffusion paths result for the carbon. Therefore, the recrystallization of the low-Cr areas occurs very quickly [8, 9].

The aim of the following study was to investigate the microstructure of heat-resistant P91 and CB2 flux-cored wire weld metals. The formation and development of inhomogeneities in the weld metal would be explained and described in detail. Effects of inhomogeneous microstructures on the mechanical properties of the weld metal would be discussed. Finally, possibilities for improving weld metal homogeneity would be investigated and evaluated.

## 2 Approach and work plan

The investigations carried out are composed of four blocks. First, a creep-damaged weld (Grade CB2) was examined regarding its damage behaviour. In a second block, welded samples (Grades P91 and CB2) were metallographically examined and evaluated in as-welded as well as heat-treated condition. The main focus was on the microstructure of the weld metals and their influence on the creep properties. Within the third block, the formation mechanisms of microstructural inhomogeneities were cleared. Finally, within the fourth block, test welds were conducted to optimize the microstructure of the weld metals.

## 3 Methods and materials

### 3.1 Methods of material analysis

After cold extraction of selected areas and subsequent hot embedding (phenolic resin with carbon addition, electrically conductive) of the samples, a wet grinding was carried out using SiC abrasive paper up to grit number #2400 (average grain diameter 10  $\mu\text{m}$ ). Subsequently, the samples were polished with diamond suspensions (particle sizes between 6 and 1  $\mu\text{m}$ ) and colloidal silicon dioxide suspension (particle size 0.02  $\mu\text{m}$ ).

For macro-sections, a grain area etching according to *Adler* was used to visualize various structural areas in the welded joints. Furthermore, a *modified Lichtenegger-Bloech* colour etching was used for micro-sections. The compositions of both etchants are given in Table 1.

For the characterization and evaluation of the microstructures of the welds, mainly light microscopic methods were used. Both macroscopic and microscopic images were taken.

Scanning electron microscope (SEM) studies were performed on selected samples to characterize their microstructure. Furthermore, energy dispersive X-ray spectroscopy (EDX) point measurements as well as line scans and mappings were conducted to determine the distribution of various elements in welding consumables and weld metals.

### 3.2 Hardness measurements

For all hardness measurements, a fully automatic hardness tester was used, which allowed test loads between 0.01 and 10 kgf. The hardness tests were carried out according to the

**Table 1** Chemical compositions of etchants

Etchant	Composition
<i>Adler</i>	Water, hydrochloric acid, Iron (III) chloride, $\text{ClCuH}_4\text{N}$
<i>Modified Lichtenegger-Bloech</i>	Water, $\text{NH}_4\text{HF}_2$ , $\text{K}_2\text{S}_2\text{O}_5$

Vickers method and were carried out according to DIN EN ISO 6507-1:2006–03.

### 3.3 CB2 creep sample

The investigated creep sample – provided by a project partner – was taken from a test weld of the heat-resistant cast material CB2. As filler material, a matching rutile-basic CB2 flux-cored wire (9Cr-1.5Mo-1Co) was used for this weldment. Following relevant details, regarding the welding process and the performance of the creep test are listed. Further information about the properties of the CB2 flux-cored wire and the weld metal properties can be found in [12, 13].

- Manual flux-cored arc welding (ISO 4063 — 136)
- Welding current, 230–250 A
- Welding voltage, approx. 27–29 V
- Layer structure, 2 beads per layer
- Shielding gas, Ar + 18% CO<sub>2</sub>
- Preheating, 200 °C
- Interpass temperature, max. 250 °C
- Post weld heat treatment, 730 °C / 12 h
- Creep test, 625 °C / 120 MPa – fractured after 27,000 h

### 3.4 Welding consumables and welding experiments

For welding experiments, commercially available flux-cored wires of Grade 91 (EN ISO 17634-A: T ZCrMo9VNb P M21 1 H5 and AWS A5.36: E91T1-M21PY-B91-H4) and Grade CB2 (EN ISO 17634-A: T ZCrMoCo9VNbNB P M21 1 and AWS A5.36: E91T1-M21PY-G) were used. Both slag-forming flux-cored wires had a rutile-basic filling. Table 2 gives the nominal chemical composition of flux-cored wire weld metals. Both flux-cored wires were manufactured using a low- or non-alloyed metal strip, which was verified by EDX element analysis in the outer metallic sheath of the flux-cored wires. As an example, Fig. 1 shows the result of an EDX-analysis for the P91 flux-cored wire. Consequently, a relatively high percentage of important alloying elements like Cr and Mo have to be contained in the powder filling of the investigated flux-cored wires in order to guarantee the requirements of the chemical composition of the flux-cored wire weld metals.

**Table 2** Nominal chemical composition of flux-cored wire weld metals in wt.-%

C	Si	Mn	Cr	Mo	Co	Ni	V	Nb	B	N
<i>P91</i>										
0.1	0.2	0.7	9.0	1.0	–	0.2	0.2	0.04	–	0.04
<i>CB2</i>										
0.12	0.2	0.9	9.0	1.5	1.0	0.2	0.2	0.03	0.006	0.02

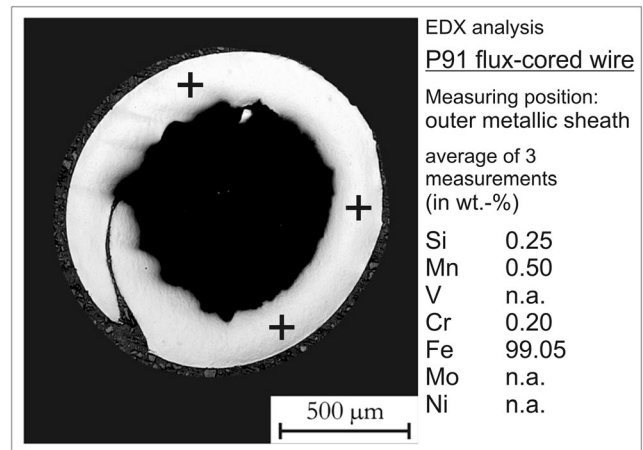


**Fig. 1** Micrograph and chemical analysis (EDX measurement) of the P91 flux-cored wire

In welding experiments, multi-layer weld pads were produced on low-alloyed steel plates (10 mm in thickness) using stringer bead technique. The weld pads consisted of six layers to eliminate a mixing of the weld metal with base material. For further investigations, only pure P91 and CB2 weld metals from the top three layers were used. Parameters regarding the manual FCAW process (ISO 4063 — 136) used are given in Table 3.

## 4 Results and discussion

### 4.1 Investigation of CB2 creep sample

Microstructural analysis showed that the fracture of the CB2 creep sample occurred within the HAZ. The distance to the fusion line was between 1 and 1.5 mm. The fracture pattern showed a comparatively small deformation or constriction. The fracture of the sample resulted from the formation of creep voids, which already grew together in the fracture area to form void chains and cracks.

**Table 3** Welding parameters used for the flux-cored wires

	P91 filler wire	CB2 filler wire
Shielding gas	Ar + 18% CO <sub>2</sub>	Ar + 18% CO <sub>2</sub>
Gas flow	18 l/min	18 l/min
Wire feed rate	10.5 m/min	10.5 m/min
Welding current	240–270 A	240–270 A
Welding voltage	28–30 V	28–30 V
Current type	DC (+)	DC (+)
Welding speed	24–30 cm/min	24–30 cm/min
Welding position	ISO 6947 - PA	ISO 6947 - PA
Preheating	200 °C	200 °C
Interpass temp.	300 °C	250 °C
PWHT	760 °C / 4 h	730 °C / 4 h

Within the investigated CB2 creep sample, different degrees of damage could be determined. In the area of the coarse-grained HAZ (CGHAZ), adjacent to the fusion line, no damage in the form of cavities or cracks was visible. The creep damage is limited to the fine grain (FGHAZ) and intercritical range (ICHAZ) of the HAZ. The damage pattern and the distance to the fusion line corresponded to the Type IV mechanism that is typical for martensitic 9% Cr steels.

It became evident that the base material was significantly more damaged than the weld metal. Creep voids were visible, which had formed primarily along former austenite grain boundaries. Only isolated voids inside the prior austenite grains were recognizable. The damage pattern within the CB2 base material thus corresponds to the typical damage course in high-temperature resistant 9% Cr steels. In contrast, apart from isolated voids, which could not be clearly attributed to the creep load, the weld metal did not show any remarkable or critical creep damage.

Within the microstructure of the creep-damaged CB2 weld metal, inhomogeneities, which sometimes extend over a length of 1 to 2 mm, could be visualized, see Fig. 2a (top). It became clear that there is a non-martensitic microstructure and a marked reduction in the number and density of precipitates in these bright areas. Furthermore, several creep voids are recognizable, which have formed in the region of the illustrated inhomogeneity. This leads to the assumption that these inhomogeneities tend to creep faster than surrounding martensitic areas. Heavily altered mechanical properties within the inhomogeneous regions can also be confirmed by microhardness measurements exemplified in Fig. 3. While the hardness in the surrounding weld metal is about 225 HV 0.05, the interior of the inhomogeneity has only about 150 HV 0.05. The low hardness values and the microstructure shown indicate a ferritic microstructure.

In addition to the almost precipitation-free inhomogeneities, band-shaped areas that have a visibly greater precipitation density than the surrounding weld metal were also found, see Fig. 2b (below). On closer inspection, it is noticeable that in Fig. 2b homogeneous areas of weld metal alternate with areas of reduced (bright) and high precipitation density (darker). The increased number of precipitates in the dark seams could be confirmed by microhardness measurements. Due to the higher precipitation density, these zones have a microhardness slightly increased by about 50 HV 0.05.

Clearly visible and extensive inhomogeneities were present in the weld metal of the investigated CB2 creep sample. But at the moment it is not entirely cleared whether these inhomogeneities have an influence on the failure mechanism of the overall compound. The FGHAZ and ICHAZ seem to represent the weakest range with respect to the creep rupture strength. Thus, FGHAZ and ICHAZ form the limiting factor with regard to the service life of the welded joint.

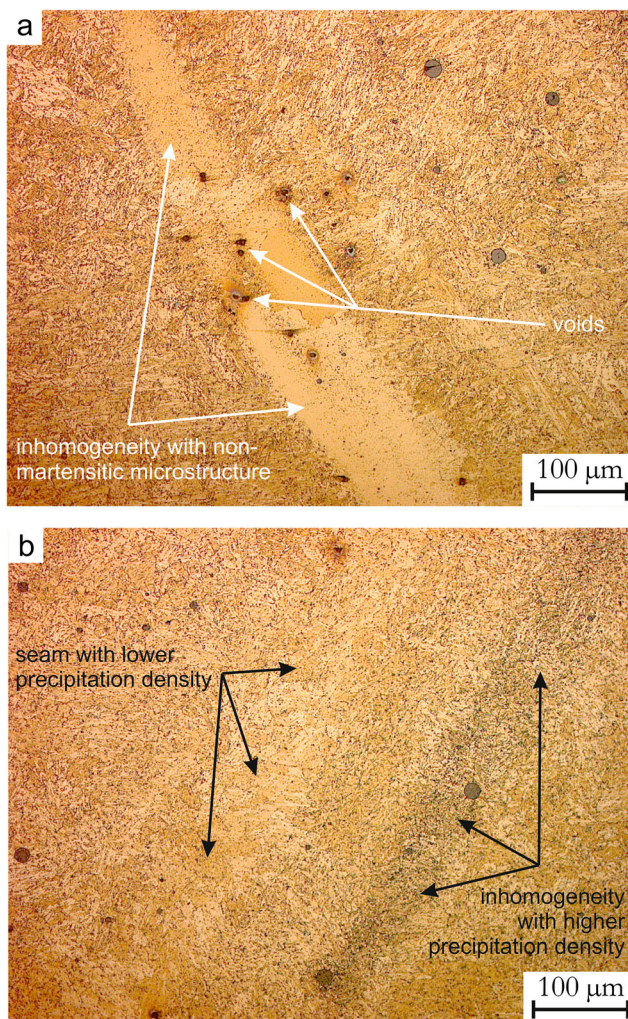


**Fig. 2** a Significant inhomogeneity (top). b Seams with varying precipitation density (below) in the weld metal of the CB2 creep sample

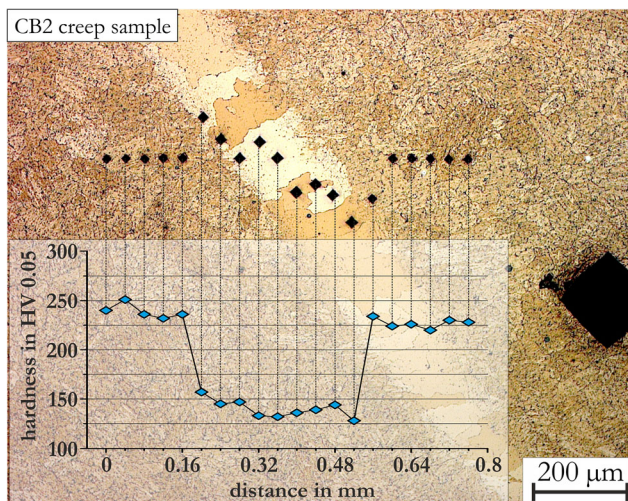


**Fig. 3** Microhardness measurements across a significant inhomogeneity within the weld metal of the CB2 creep sample

## 4.2 Investigation of P91 and CB2 weld metals

Both flux-cored wires were manufactured according to the current state of the art. To study the formation of inhomogeneous areas, the microstructures of the weld metals (P91 and CB2) were analysed in as-welded and post weld heat treated (PWHT) condition. An identical formation and development of the inhomogeneous areas in the weld metal was determined for both flux-cored wires. Therefore, the following results are described using the example of the P91 weld metal but can be transferred to the CB2 flux-cored wire as well.

Figure 4a (top) shows several weld beads of the P91 weld metal after cooling from the welding heat. Even after welding, significant inhomogeneities or zones of poor mixing in the lower region of the individual layers are clearly visible. The strip-like inhomogeneities, which appear bright in the micrograph, sometimes extend over several millimetres. In these areas, a greatly changed microstructure compared to the

surrounding weld metal is visible. The general martensitic structure of the weld metal is interrupted by the bright strip-like inhomogeneities. Due to the rapid solidification and cooling of the weld metal, the microhardness fluctuates strongly, whereby no clear tendency can be assigned to the different microstructure areas with regard to an increase or a decrease in hardness, see Fig. 5a (top). The hardness values and the etching behaviour (due to Cr enrichment as will be shown later) indicate that the bright areas could be a mixture of martensitic areas and zones that are partially solidified by solid solution strengthening.

After tempering of the weld metal (760 °C/4 h), extensive inhomogeneities are also visible, see Fig. 4b (below). In contrast to the upper image (Fig. 4a), the course and extent of the inhomogeneities can be seen more clearly. This can be justified by the fact that, in particular, the stabilizing precipitates are predominantly formed during the tempering process and that the microstructure evolves its final structure. Therefore,

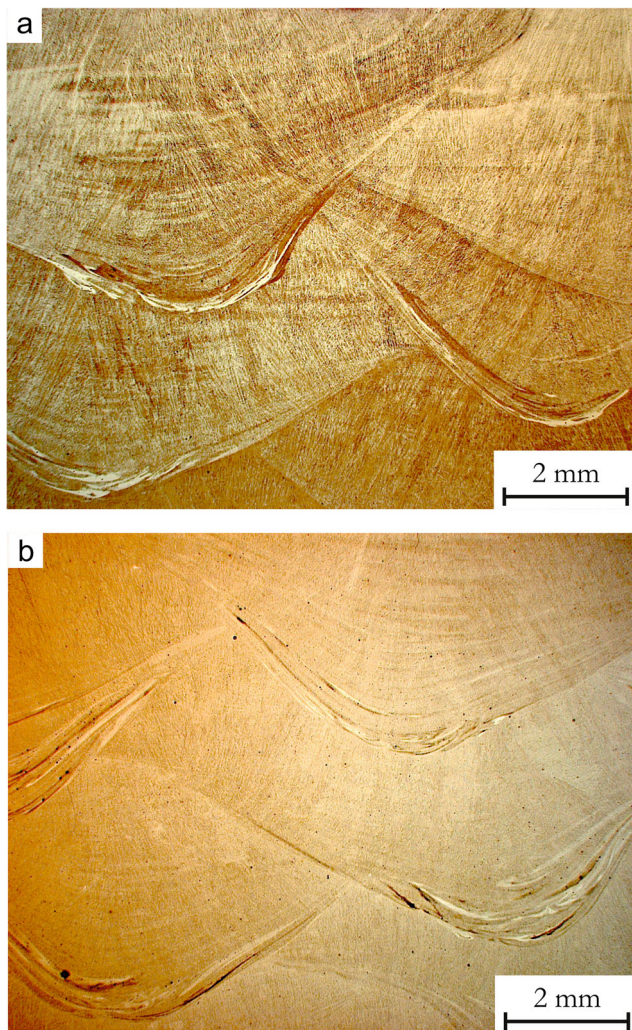


**Fig. 4** **a** Microstructures of P91 flux-cored wire weld metal in as-welded (top). **b** PWHT (below) condition showing clearly visible inhomogeneous areas

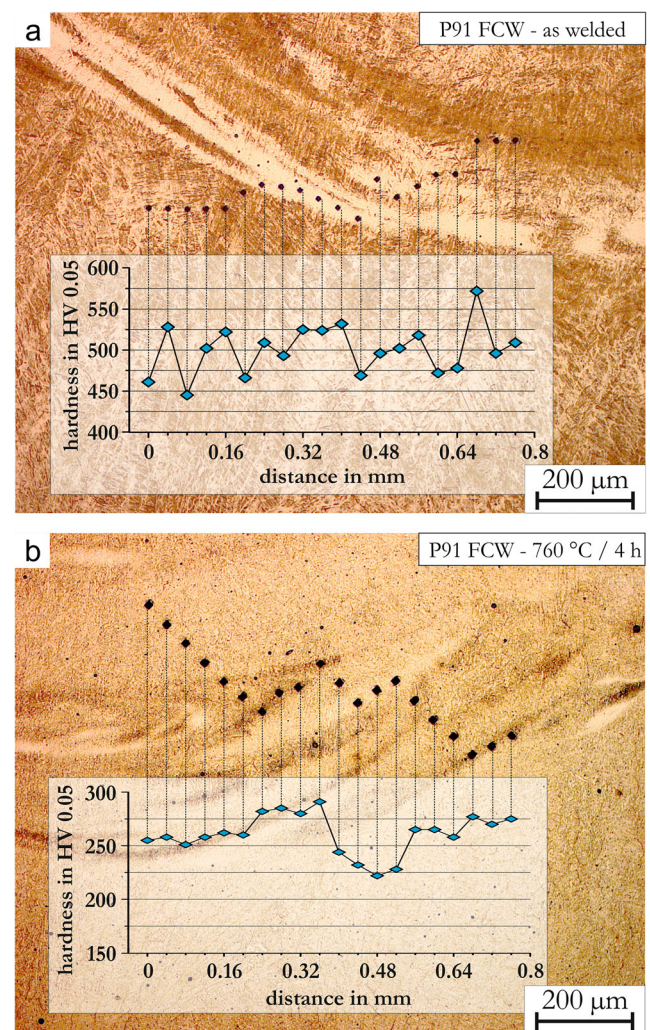


**Fig. 5** Microhardness of strip-like inhomogeneities in P91 flux-cored wire weld metal. **a** As-welded condition (top). **b** Tempered condition (below)

modified microstructures can be made more visible and differentiated in the tempered state. This optical effect can be attributed to a changed precipitation density compared to homogeneous weld metal areas. The detailed micrograph in Fig. 6a (top) shows that within the bright inhomogeneities significantly fewer precipitates than in the rest of the weld metal are formed. Martensite laths or martensitic structures, as in the surrounding matrix, are not visible. In the dark areas, the number of precipitates is clearly increased. The presence of delta ferrite has also been observed in several of these dark areas, see Fig. 6b (below). The inhomogeneous areas illustrate that the distribution of the alloying elements is disturbed.

The measured line scan in Fig. 5b (below) shows that the hardness within the bright inhomogeneities decreases very strongly during and after the PWHT. Depending on the characteristics of these bright stripes, different values are measured, although the hardness is always lower than in the surrounding weld metal areas. In some cases, a microhardness

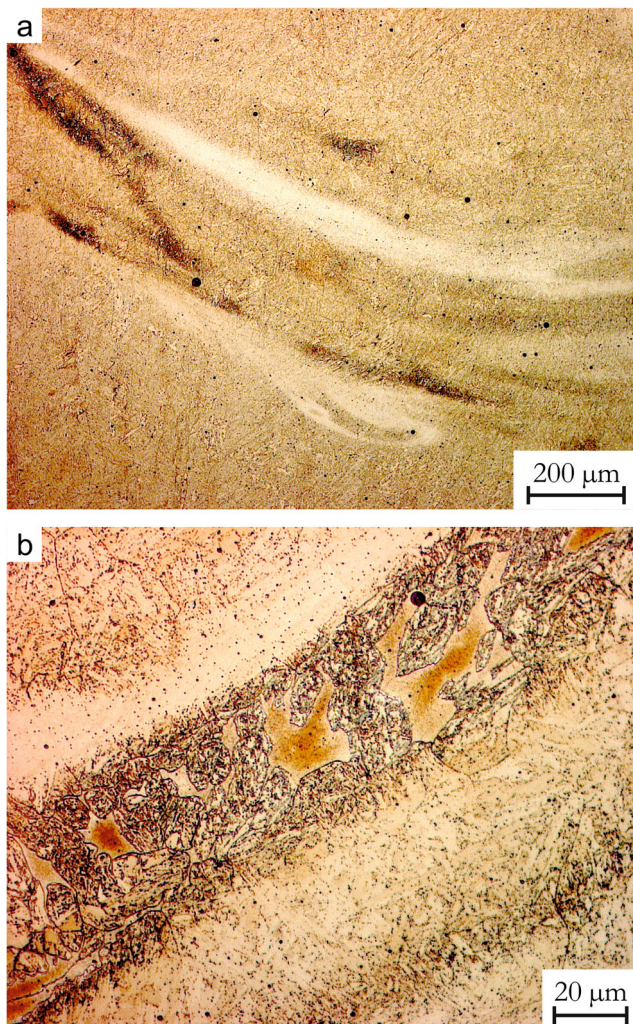
significantly below 200 HV 0.05 was determined. This indicates that some ferritic structures may be present in these areas. Secondly, it can be stated that the lower the precipitation density inside the bright inhomogeneities and the more pronounced the inhomogeneous zones, the lower the hardness is. Figure 5b also shows that the darker areas have a higher microhardness, which correlates with their higher precipitation density. Such large inhomogeneous areas are present in almost all individual weld beads of the P91 and CB2 flux-cored wire weld metal. In connection with the micro-sections in Fig. 6a and b, it can be seen that in a comparatively large area within the individual weld beads, different band-shaped areas alternate in an unordered sequence. In addition to the microstructural differences, the fluctuations in the measured hardness values indicate varying mechanical properties, such as strength and toughness, in the various strip-shaped zones. It is highly probable that the different microstructural regions also exhibit toughness properties deviating from those of the homogeneous matrix. In particular, the darker (harder) seams could exhibit comparatively low ductility and thus influence the notched impact strength of the weld metal.

Although inhomogeneous areas are clearly recognizable within the investigated flux-cored wire weld metals, they seem to influence the creep rupture strength of welded joints (in case of P91 and CB2) marginally. Welded joints of P91 and CB2 in general exhibit damage behaviour according to the Type IV mechanism. The literature does not report any failure within the weld metal under the normal operating conditions typical for power plants. The creep-damaged CB2 sample described above, which shows distinct inhomogeneities within the weld metal, supports the assumption that the inhomogeneous areas in case of P91 and CB2 do not negatively influence the creep rupture strength of the entire joint.

### 4.3 Formation of microstructural inhomogeneities

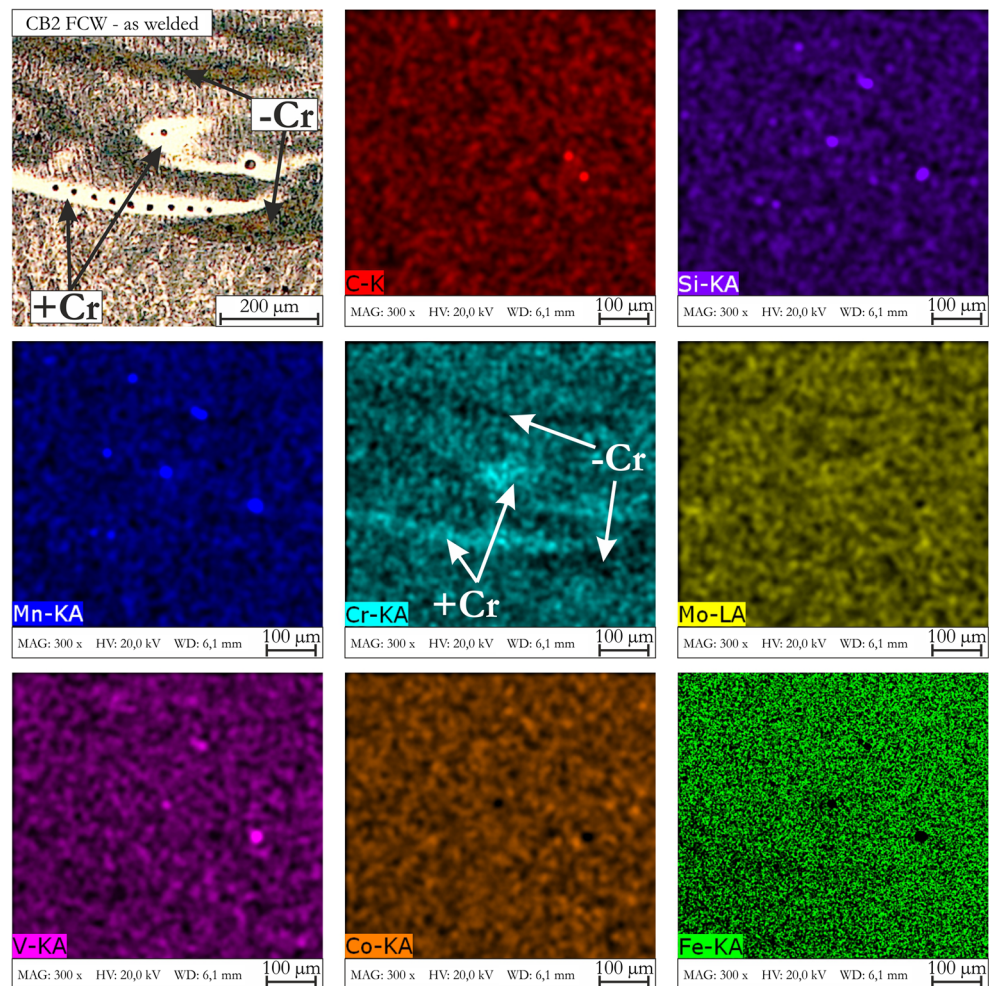
In order to draw conclusions about the development of the described inhomogeneities, selected samples were examined by EDX measurements. EDX mappings were performed to obtain qualitative results regarding the element distribution in the inhomogeneous regions.

Figure 7 shows an EDX measurement in the CB2 flux-cored wire weld metal in as-welded condition. Some hardness impressions are still visible. In the measured area, Cr in particular shows an uneven distribution. It can be seen that the bright inhomogeneities that developed after the solidification of the melt are rich in Cr. The comparatively high hardness values measured in this zones (shown in Fig. 5a using the example of the P91 weld metal) could thus be attributed to hardening due to the increased Cr content. Somewhat above the Cr-rich zone, a zone with less Cr than the surrounding weld metal is also visible, which appears as a dark brown seam in the light



**Fig. 6** a Inhomogeneities within the P91 flux-cored wire weld metal after PWHT 760 °C/4 h (top). b Detail of inhomogeneities containing some delta ferrite (below)

**Fig. 7** Qualitative element distribution in an inhomogeneous area within the CB2 flux-cored wire weld metal (as-welded)

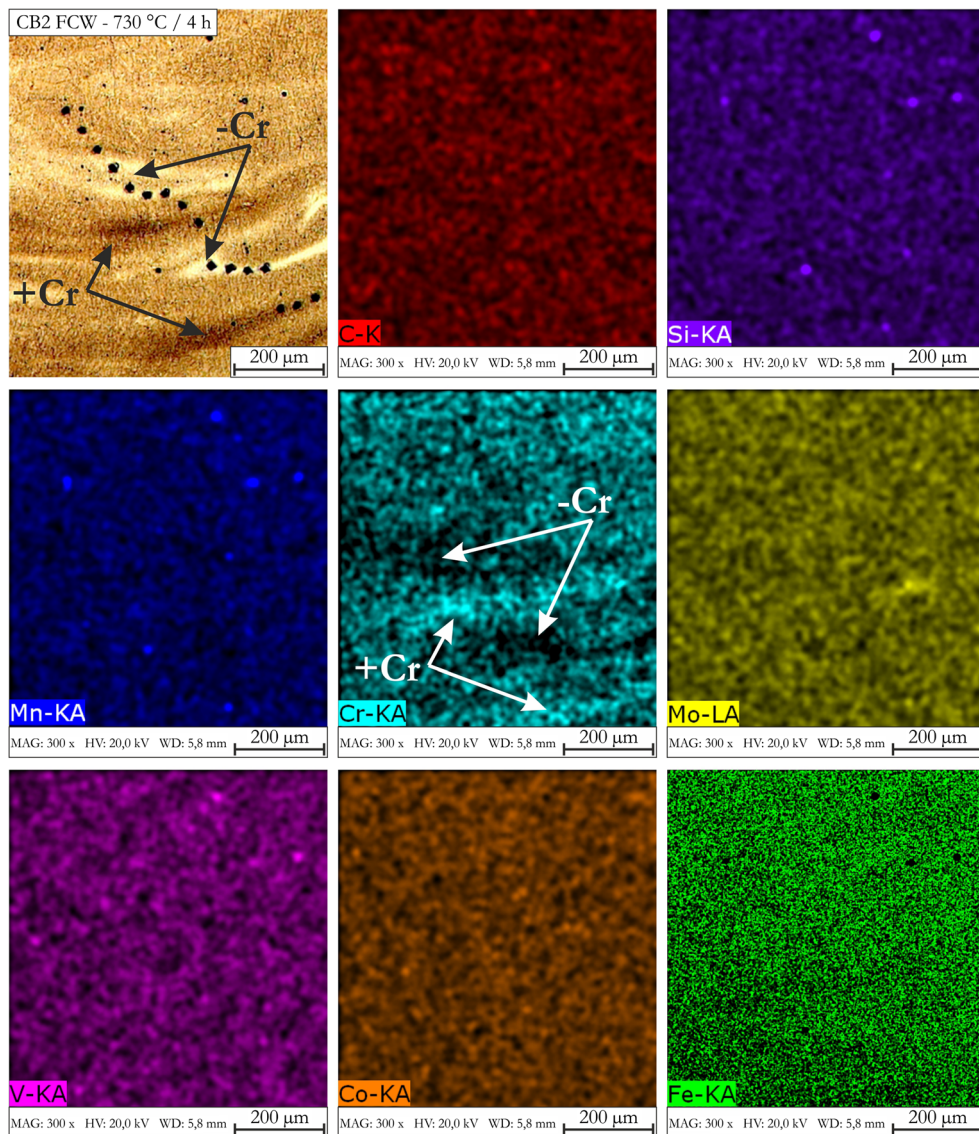


microscope image. The dark brown discoloration of the Cr-poor inhomogeneities in this case results from a strong over etching of the sample, which makes these zones visible. With a lighter etching, the Cr-poor seams in as-welded state would hardly be recognizable or not at all. Because of poor mixing, low-Cr and Cr-rich inhomogeneities occur in addition to weld metal areas consisting of the chemical “nominal composition”. Compared to Cr, the also large atomic elements Co and Mo show a more homogeneous distribution. Some round slag particles with Si, Mn and V content are visible. Nickel and carbon do not show any abnormalities in the measurement shown. However, it must be noted that the measurement of these two alloying elements must be evaluated with caution using the EDX method due to the small proportions in the weld metal. The EDX measurement result of the P91 flux-cored wire is qualitatively similar to the result of the CB2 flux-cored wire described above. This measurement also showed that in particular there is a strong uneven distribution of the element chromium within the inhomogeneous weld metal zones. The EDX measurements show that the general assumption that gas metal arc welding with flux-cored wires,

due to the high temperatures in the arc, melts and homogeneously distributes all powdery filler constituents is not correct in the case of the investigated high-alloyed filler metals.

Figure 8 shows an EDX measurement result within an inhomogeneous region within the tempered CB2 weld metal. The image shows brightly appearing and very dark appearing inhomogeneities. These contrasts result from the already described differences in precipitation density in these seams. This was clarified by already described light microscopy and confirmed by microhardness measurements. In comparison to Fig. 7, however, a different picture now emerges with regard to the element distribution. As the EDX mappings show, there is a slight Cr depletion within the brightly appearing inhomogeneities – in contrast to the as-welded condition. On the other hand, the dark and precipitation-rich inhomogeneity shows a distinctly (in part strongly) pronounced increase in the Cr content in comparison with the surrounding matrix. It can be assumed that Cr hardly diffuses during tempering (730 °C/4 h). This means that the Cr and precipitation-rich seams are those inhomogeneities, which appeared bright to white in the light microscopic micrograph before the

**Fig. 8** Qualitative element distribution in an inhomogeneous area within the CB2 flux-cored wire weld metal (PWHT: 730 °C/ 4 h)



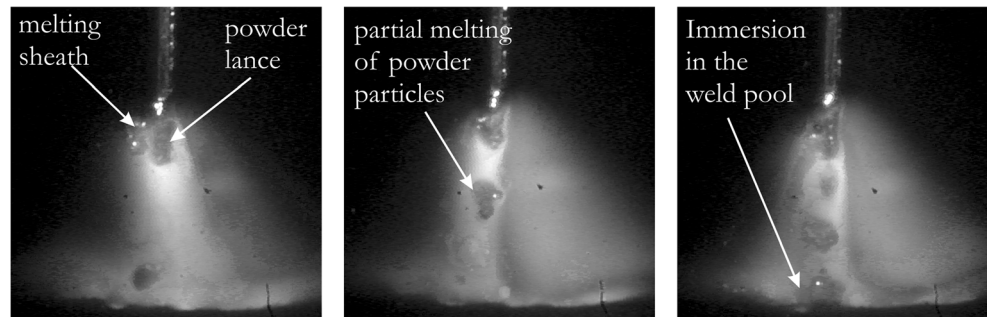
PWHT. Although the Cr-poor inhomogeneities were already present after welding, the extent of the now precipitation-poor and bright inhomogeneities (“white bands”) only becomes visible because of the tempering treatment. The reason for this is the diffusion of carbon into surrounding areas with a higher Cr content during tempering. However, the carbon content of the CB2 weld metal is too low overall to make C-rich zones visible with the EDX method.

Figure 9 shows images depicting successive stages in the melting of the P91 flux-cored wire. These images were taken from video recordings taken with a high-speed camera during welding. The image on the left shows that the outer metallic sheath of the flux-cored wire melts at the arc attachment and a so-called powder lance protrudes into the arc. During welding, the powder lance is pushed further and further into the arc column and melts increasingly. In both images (left and middle), it can be seen that the melt from the sheath is much

thinner and therefore appears to be hotter. On the other hand, the powder components within the arc are heated by convection and heat conduction. Therefore, the powder column inside the arc is only partially molten. That means more time is needed to liquefy the filling components of the flux-cored wires, as can be seen in the image on the right. When immersed in the weld pool some of the powder components are not completely melted.

Figure 10 shows a scheme regarding the formation of inhomogeneities during welding using the example of the CB2 flux-cored wire (unalloyed outer metallic sheath). As the high-speed camera images showed, outer metallic sheath and powder filling are almost melting separately. This results in two partial melts with different flow properties. The melt of the outer metallic sheath (“melt A”) becomes hotter and thus has a lower density and viscosity (thinner and more flowable). The complete melting of the powder particles takes place in the

**Fig. 9** Melting of the P91 flux-cored wire during welding (taken from video recordings using a high-speed camera)

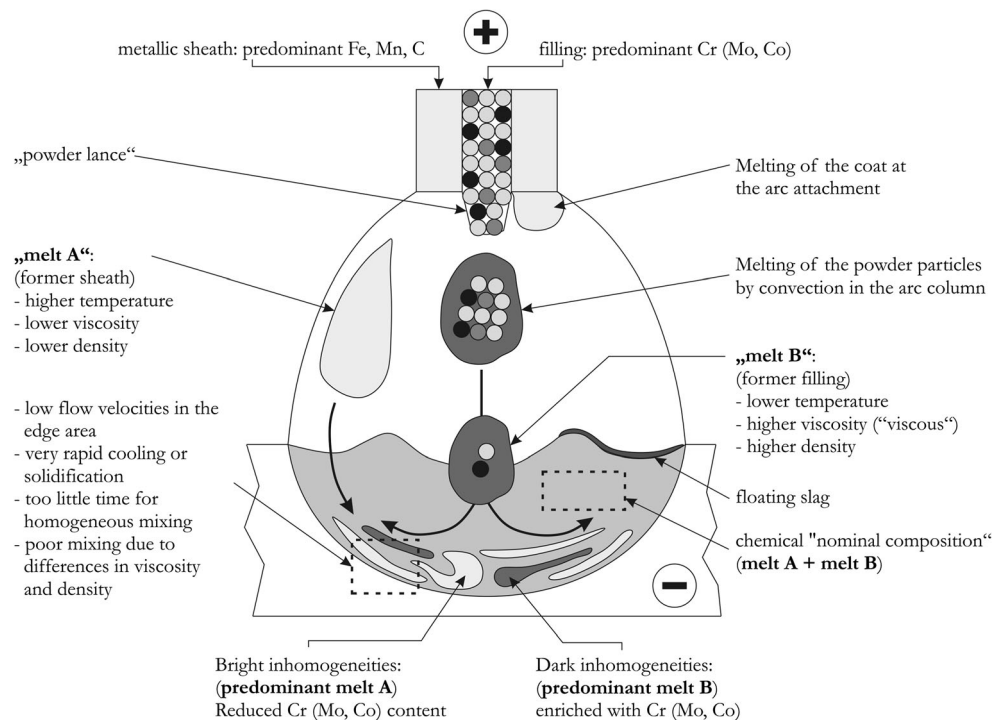


weld pool. Since a lower temperature of the molten powder (“melt B”) can be assumed, this melt has a higher density and viscosity (thicker and less flowable). This leads to a tendency for “melt B” to sink within the weld pool (buoyancy forces). In addition, their different densities and flow properties impair the mixing of both melts. The inhomogeneities occur at the edges of the weld metal. In these areas, the flow velocity of the melt is lower, which makes mixing more difficult. In addition, the weld pool temperature is lowest there or the cooling rate and cooling speed are highest there. This means that less time is available for diffusion movements than in the centre of the weld pool. The higher temperatures in the middle of the weld pool cause an approximation of the viscosity and density differences of the “melts A and B” as well as an extension of the solidification time, whereby their mixing is clearly improved. The movements within the weld pool, such as Marangoni convection or movements induced by Lorentz forces and arc pressure are not sufficient to produce a homogeneous melt in the edge area. The fact that the inhomogeneities in the

investigated flux-cored wire weld metals can be attributed to an uneven mixing of two “partial melts” can be demonstrated as follows. Elements that show depletion in light inhomogeneities (reduced precipitation density) are increasingly present in dark inhomogeneities (larger precipitation density).

Figure 11 shows a scheme of the processes during tempering and under creep loading. In the Cr-rich inhomogeneities, which appear bright after welding, martensite formation during cooling can be influenced by the enriched Cr content in these areas and the low-C content of the overall weld metal (0.1 wt.-%). During tempering, carbon from the surrounding matrix diffuses into the Cr-rich zones, causing the formation of numerous precipitates. Furthermore, delta ferrite – which was already present after welding – remains and is stabilized by the higher Cr content. Around the Cr-rich seams, “light-coloured edges” develop due to carbon diffusion during tempering, which become poor of precipitates or in which hardly any precipitates are formed. During tempering, the martensitic structure formed around the Cr-rich seams after welding is

**Fig. 10** Scheme regarding the formation of inhomogeneities during welding using flux-cored wires (Grades P91, CB2, unalloyed sheath)



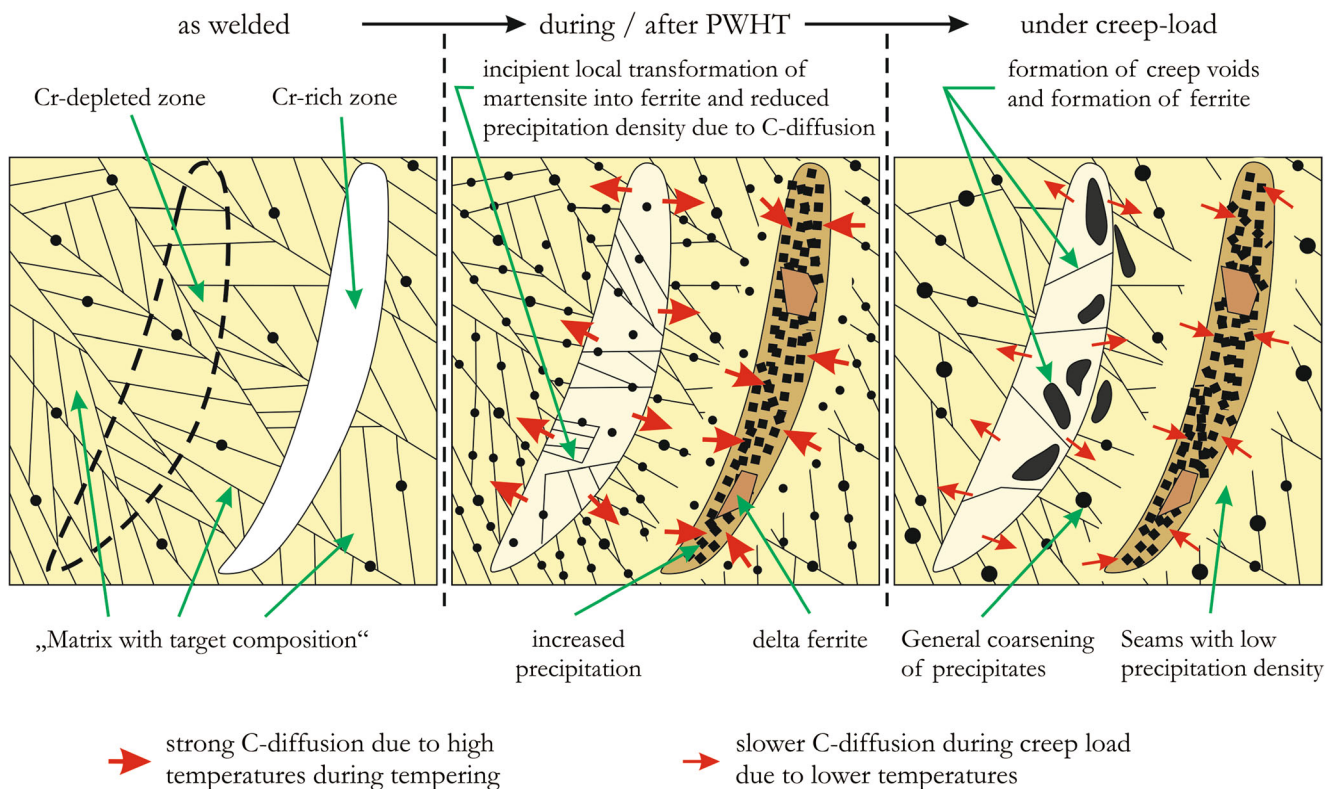


**Fig. 11** Diagram of processes inside and outside the inhomogeneities during tempering and under creep load

partially transformed, since carbon diffuses toward the higher Cr content and the martensite therefore becomes ferrite. Under creep loading, C diffusion continues to progress. This means that the dissolution of precipitates and the transformation of tempered martensite around the Cr-rich inhomogeneities continue, resulting in the gradual formation of carbide-free ferrite. Creep damage in the form of cavities could occur both inside and outside the precipitation-rich inhomogeneities. On the one hand, the resulting ferritic microstructure has a comparatively low creep strength. On the other hand, precipitates are places where cavities are formed because of dislocation accumulation, and creep voids can thus be formed. Within the creep-damaged CB2 sample, however, hardly any damage was found in these precipitation-rich inhomogeneous zones.

As already mentioned, after welding the Cr-depleted inhomogeneous zones are hardly detectable by light microscopy, which is illustrated by the dashed line in the left picture of the scheme (Fig. 11). In the “as-welded” state, despite a reduced Cr content, hardly any difference in the formation of the microstructure within these zones is visible. Electron probe micro analysis (EPMA) measurements within creep-damaged P91 weldments (investigated parallel to the presented study) had shown that the Cr content in these zones is about 8–8.5 wt.-%, see Fig. 12. This is sufficient to form a martensitic structure when cooling down from the welding heat. The expansion of the inhomogeneities only becomes visible after tempering, because precipitates have formed and the altered microstructure provides an optical

contrast. Although the gradient of the Cr content is only about 0.5–1.5 wt.-%, during tempering carbon diffuses from the Cr-depleted zones into the surrounding weld metal areas where the Cr content is within the target range of around 9 wt.-%. As a result, during high temperature, tempering the martensite in Cr-depleted areas is gradually transformed into ferrite, and only a few precipitates are formed. These processes continue under creep loading and high-temperature service. Due to a difference in carbon activities the precipitates formed during tempering within the Cr-depleted zones are dissolved with increasing creep exposure. As a result, a carbide-free ferritic microstructure remains. Creep voids arise inside and around the inhomogeneities with low-Cr content.

#### 4.4 Optimization of weld metal microstructure

By varying the welding parameters, an attempt was made to exert greater influence on the temperature characteristics within the arc and the movements of the weld pool. The wire feed rate was varied between 9.5 and 12.5 m·min<sup>-1</sup>. The tests should show whether it is possible to suppress the formation of inhomogeneous areas in the weld metal by increasing or reducing the welding performance.

However, it was impossible to suppress the formation of inhomogeneous zones. In all weld metals, distinct inhomogeneities with lower and higher precipitation densities were visible. With increasing welding power, the inhomogeneous

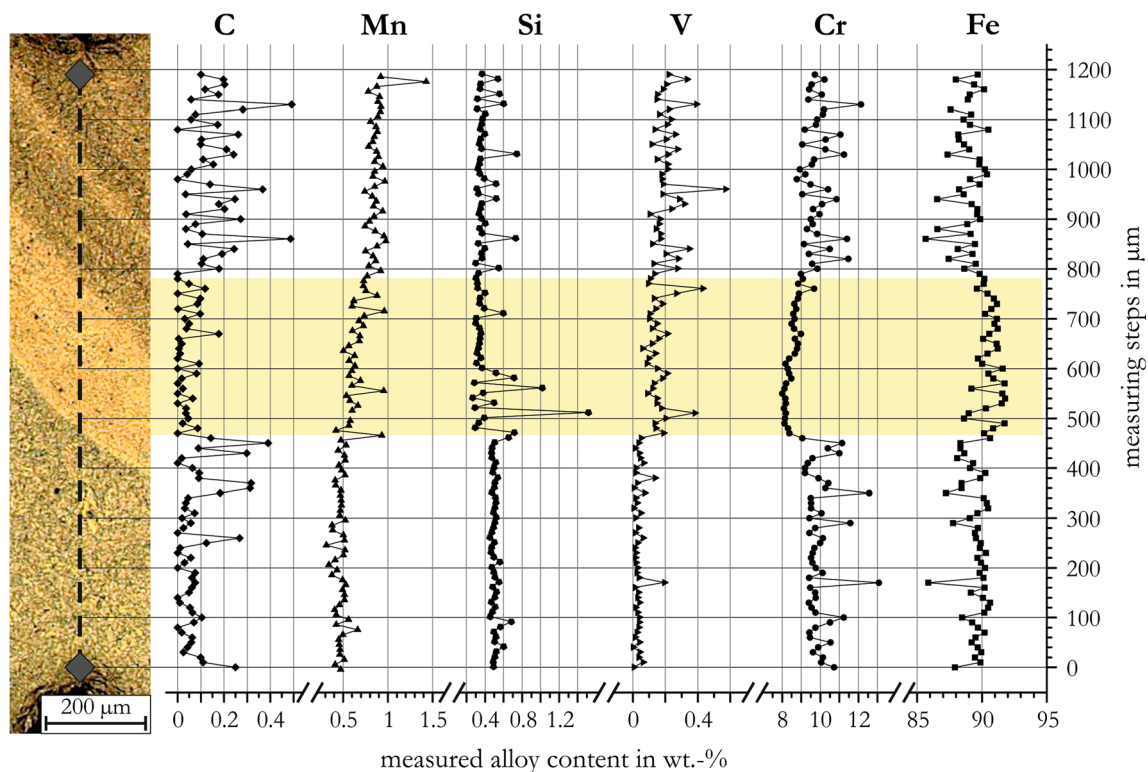


**Fig. 12** EPMA measurement of alloying elements over an inhomogeneity within a creep-damaged P91 weld metal

areas, which arise in the lower third of the weld beads, seem to become larger and more extensive. In addition, the proportion of dark inhomogeneities (rich in precipitates), which contain significant amounts of delta ferrite and poorly melted powder, tends to increase.

In order to improve the mixing of the weld pool during flux-cored arc welding and to avoid inhomogeneous areas, comparatively low wire feed rates would have to be used. However, low wire feed rates could affect the short and transition arc range, which would increase the risk of defects in the weldments. On the other hand, the achievable productivity and desired economic efficiency of the flux-cored wires would be impaired. By reducing the welding parameters, a reliable avoidance of inhomogeneities could not be achieved. Therefore, one possibility to avoid inhomogeneous areas within the weld metals is to modify the production of the flux-cored wires. Large alloying elements – especially Cr, Mo and Co – should be shifted into the outer metallic sheath of the P91 and CB2 flux-cored wires as much as possible. That means high-alloyed metal sheaths should be used as starting product for the industrial manufacturing of the investigated flux-cored wires. If the main alloying elements (Cr, Mo, Co) are already dissolved in an alloy these elements no longer have to be melted in the form of powder particles. Therefore, the mixing of the weld pool – and consequently the homogeneity of the entire weld metal – should be significantly improved.

## 5 Conclusions

It is important to note that the inhomogeneities found within the investigated CB2 and P91 weld metals, according to current knowledge, have no negative impact on the creep rupture strength of the entire welded joints. Although significant microstructural changes can be observed in the form of ferrite formation (within Cr-poor and around Cr-rich inhomogeneities) and precipitation accumulation (within Cr-rich inhomogeneities), the HAZ still appears to be the weakest link of the weld joints (Type IV mechanism). From the current perspective, there are no concerns with regard to the safety of existing or operating plants. However, the development of steel grades like MARBN (9Cr3W3CoVNbBN) or P93 may increase the significance of the investigated inhomogeneities. Such creep resistant steels have a higher creep rupture strength. Further, these modern steel grades are specifically alloyed to suppress the Type IV mechanism by stabilizing the HAZ. The suppression of the fine grain zone could cause a shift of the preferred fracture location to other regions of the weld joints. Further, this strengthening of the weakest link within the weld joints could result in greater stress on the weld metal, which in turn could lead to accelerated damage in the inhomogeneous regions. With a view to welding consumable developments for such modern creep strength enhanced steels, greater attention should therefore be paid to the homogeneity and microstructure of the weld metal.

The investigations showed that light microscopy and a suitable etching process – in this case a modified Lichtenegger-Bloech etching – can be used to precisely check the microstructural homogeneity. Using the etching method described in this study a detection of existing inhomogeneous areas within the weld metal is possible for heat-resistant 9% Cr steels like P91 and CB2, both after welding and after PWHT.

Inhomogeneous areas are already present after welding. Their formation takes place already during the solidification of the weld metal. After the usual PWHT, the inhomogeneities appear as bright strip-like bands (predominantly ferritic, reduced precipitation density, reduced hardness) and dark seams (tempered martensitic, high precipitation density, higher hardness). Within the dark inhomogeneities, also delta ferrite contents were frequently found.

The formation of inhomogeneities is due to poor mixing of the weld pool, which is caused by insufficiently melted filling components. At the arc attachment, outer metallic sheath and powder filling melt apart from each other. As a result, the temperature and temperature distribution within the materials is different. The resulting differences in viscosity and density of the separate melts (sheath and filling) as well as slow flow velocities at the edge of the weld pool contribute to these phenomena.

In particular, bright inhomogeneous seams, detectable after welding using Lichtenegger-Bloech etching, show increased Cr contents. If further main alloying elements are added via the filling, these can also occur within the bright Cr-rich inhomogeneities after welding.

Due to a lower carbon activity within the Cr-rich inhomogeneities, more precipitates are formed in these seams during PWHT than in the rest of the weld metal. In tempered condition, this makes them visible as dark, strip-shaped inhomogeneities in the light optical micrograph. Further, due to C diffusion edges form around the Cr-rich seams, in which martensite transforms to ferrite and precipitates are gradually dissolved.

The inhomogeneities appearing bright in the tempered state and low in precipitation density are hardly or not at all visible after welding, since the Cr content is only slightly lower than in the surrounding weld metal, and thus a martensitic microstructure is initially formed. During PWHT, the incipient C-diffusion into the surrounding weld metal with targeted Cr content of around 9 wt.-% causes a significantly reduced formation of precipitates within the inhomogeneities with lower Cr content. In addition, a clear recovery and partial transformation of the martensitic microstructure is already beginning in these seams.

Under creep loading, decelerated C diffusion continues, resulting in increased precipitation and faster growth of precipitates within the Cr-rich inhomogeneities. In the Cr-poor inhomogeneities, precipitates dissolve continuously and the former martensitic structure gradually transforms to a carbide-free ferritic structure.

The investigations and theoretical considerations show that Cr and its homogeneous distribution are important with regard to the long-term stability of the weld metal microstructure. Even slight local changes in the Cr content, both enrichments and reduced proportions, cause diffusion processes, which can lead to creep damage during long operating periods.

By reducing the welding performance or the wire feed rate, the melting behaviour of the flux-cored wires can be influenced, and thus the formation of inhomogeneities can be reduced. However, a complete avoidance of inhomogeneous areas cannot be achieved in this way. Increasing wire feed rates led to a deterioration of the weld metal homogeneity and an increased occurrence of inhomogeneities.

The higher the welding or melting performance, the more poorly melted powder residues originating from the filling occur within the inhomogeneities. This can be attributed to the increasing quantity of powder, which does not melt in sufficient time as the wire feed increases. This melting problem worsens increasingly, the greater the proportion of alloying elements added via the filling in the flux-cored wires.

Complete avoidance of inhomogeneous zones can be achieved by alloying as much as possible of the main alloying elements via the outer metallic sheath and by optimally matching the chemical compositions of the metallic sheath and the filling.

**Funding Information** Open Access funding provided by Projekt DEAL.

**Open Access** This article is licensed under a Creative Commons Attribution 4.0 International License, which permits use, sharing, adaptation, distribution and reproduction in any medium or format, as long as you give appropriate credit to the original author(s) and the source, provide a link to the Creative Commons licence, and indicate if changes were made. The images or other third party material in this article are included in the article's Creative Commons licence, unless indicated otherwise in a credit line to the material. If material is not included in the article's Creative Commons licence and your intended use is not permitted by statutory regulation or exceeds the permitted use, you will need to obtain permission directly from the copyright holder. To view a copy of this licence, visit <http://creativecommons.org/licenses/by/4.0/>.

## References

1. Parker J (2014) In-service behavior of creep strength enhanced ferritic steels Grade 91 and Grade 92 - Part 2 weld issues. *Int J Press Vessel Pip* 114–115:76–87
2. Abson DJ, Rothwell JS (2013) Review of type IV cracking of weldments in 9–12%Cr creep strength enhanced ferritic steels. *Int Mater Rev* 58(8):437–473
3. Watanabe T, Tabuchi M, Yamazaki M, Hongo H, Tanabe T (2006) Creep damage evaluation of 9Cr-1Mo-V-Nb steel welded joints showing Type IV fracture. *Int J Press Vessel Pip* 83:63–71
4. Wang X, Pan Q, Ren Y, Shang W, Zeng H, Liu H (2012) Microstructure and type IV cracking behavior of HAZ in P92 steel weldment. *Mater Sci Eng A* 552:493–501

5. Falat L, Homolová V, Čiripová L, Ševc P, Svoboda M (2017) Ageing Effects on Microstructure, Mechanical Properties and Fracture Behaviour of 9Cr-1.5Mo-1Co-VNbBN Martensitic steel Welded Joint for High Temperature Application. *Adv Mater Eng* 2017(3):1–14
6. Sakthivel T, Vasudevan M, Laha K, Parameswaran P, Chandravathi KS, Panneer Selvi S, Maduraimuthu V, Mathew MD (2014) Creep rupture behaviour of 9Cr-1.8W-0.5Mo-VNb (ASME grade 92) ferritic steel weld joint. *Mater Sci Eng A* 591:111–120
7. Zhang Z, Golding M, Bouillot C (2016) Development of matching welding consumables for Boron/Cobalt alloyed 9% Cr-Mo steels and the weld metal properties, *Adv Mater Technol Fossil Power Plants*, Proceedings from the 8th International Conference (EPRI 2016), 2016 Albufeira, Algarve, Portugal, 11.-14. Oktober, pp 940–951
8. Zhang Y (2009) Changes in microstructure and mechanical properties of P91 weld metal during creep, doctoral thesis, University of Nottingham, Nottingham, UK
9. Zhang Y, Shipway PH, Boue-Bigne F (2009) Characterisation of creep-weak zones (white bands) in grade 91 weld metal. *Sci Technol Weld Join* 14(6):542–548
10. Allen DJ, Harvey B, Brett SJ (2005) FOURCRACK Advanced coal-fired power plant steels - avoidance of premature weld failure by 'type IV' cracking. Project summary 304, Department for Trade and Industry, UK
11. Savage WF, Nippes EF, Szekeres ES (1976) Study of weld interface phenomena in a low-alloy steel. *Weld J* 55:260–268
12. Baumgartner S, Posch G, Mayr P (2012) Welding advanced martensitic creep-resistant steels with Boron containing filler metal. *Weld World* 56(7–8):2–9
13. Baumgartner S, Holy A, Schuler M, Saric A, Schnitzer R, Enzinger N (2014) Properties of a creep resistant 9Cr-1.5Mo-1Co cast steel joint welded with a matching flux-cored wire. *Weld World* 58:565–575

**Publisher's note** Springer Nature remains neutral with regard to jurisdictional claims in published maps and institutional affiliations.